

Research Paper

Multifunctional Polymeric Micelles for Enhanced Intracellular Delivery of Doxorubicin to Metastatic Cancer Cells

Xiao-Bing Xiong,¹ Abdullah Mahmud,¹ Hasan Uludağ,² and Afsaneh Lavasanifar^{1,3}

Received April 19, 2008; accepted June 19, 2008; published online July 18, 2008

Purposes. To develop multifunctional RGD-decorated poly(ethylene oxide)-*b*-poly(ester) based micelles and assess their pH-triggered core degradation and targeted drug release in tumor cells that overexpress RGD receptors.

Methods. Novel poly(ethylene oxide)-*b*-poly(ϵ -caprolactone) (PEO-*b*-PCL) based copolymers modified with RGD ligands on PEO and pendent functional groups on PCL, i.e., GRGDS-PEO-*b*-poly(α -benzylcarboxylate- ϵ -caprolactone) (GRGDS-PEO-*b*-PBCL) and GRGDS-PEO-*b*-poly(α -carboxyl- ϵ -caprolactone) (GRGDS-PEO-*b*-PCCL), were synthesized. Chemical conjugation of doxorubicin (DOX) to PCCL core produced GRGDS-PEO-*b*-P(CL-DOX) micellar conjugates, while GRGDS-PEO-*b*-PBCL were used to physically encapsulate DOX. For both systems, micellar core degradation, drug release, intracellular drug uptake/disposition, and cytotoxicity against B16F10 metastatic cells were investigated.

Results. The PBCL and P(CL-DOX) cores were found resistant to degradation in pH 7.2, but showed 10% and 40% loss in core molecular weight in pH 5.0 within 144 h, respectively. Preferential release of DOX and DOX derivatives from PBCL and P(CL-DOX) cores was noted in pH 5.0, respectively. The GRGDS-modified micelles showed enhanced cellular internalization through endocytosis, increased intracellular DOX release, nuclear localization, and improved cytotoxicity against metastatic B16F10 cells compared to their unmodified counterparts.

Conclusions. The results clearly suggest a promise for the development of multifunctional polymeric micelles with RGD ligand decorated shell and endosomal pH-triggered degradable core for selective DOX delivery to metastatic cancer cells.

KEY WORDS: block polymer; drug delivery; doxorubicin; micelles; poly(ethylene oxide)-*b*-poly(ϵ -caprolactone); RGD peptides.

INTRODUCTION

The effectiveness of chemotherapy in cancer treatment is significantly impaired due to non-selectivity of anticancer drugs for malignant cells. A growing body of evidence supports a great promise for nano-technology approaches in improving the outcome of cancer chemotherapy through tumor-selective drug delivery (1–4). Development of carriers endowed with tumor targeting functions will enable specific delivery of cytotoxic agent to malignant tissues, thereby increasing their local efficacy, while sparing peripheral tissue from toxic side effects of the chemotherapeutic agent.

In recent years polymeric micelles have attracted a lot of attention as efficient delivery systems for the solubilization and tumor-targeted delivery of chemotherapeutic agents after systemic administration (5,6). The unique feature that has made polymeric micelles attractive in this regard is the

flexibility of block copolymer chemistry that permits simultaneous modification of the micellar core and shell structure without one affecting the other. In the context of drug targeting, these modifications are aimed at designing polymeric micellar systems that can provide optimum disposition of the incorporated drug in the biological system, i.e., within the reach of its molecular targets in cancerous tissue and away from non-target healthy cells. Taking advantage of the chemical flexibility of core/shell structure has resulted in the development of multifunctional polymeric micelles that bear multiple targeting functionalities on an individual carrier and are expected to achieve superior selectivity for the diseased tissue (7).

The objective of this study was to develop multifunctional polymeric micelles based on RGD decorated poly(ethylene oxide)-*b*-poly(ester) block copolymers with potential for selective delivery of doxorubicin (DOX) to metastatic tumor cells. Our research group has reported on the development of novel methoxypoly(ethylene oxide)-*b*-poly(ester) based micelles, i.e., methoxypoly(ethylene oxide)-*b*-poly(α -benzyl-carboxylate- ϵ -caprolactone) (MePEO-*b*-PBCL) and MePEO-*b*-poly(α -carboxyl- ϵ -caprolactone) (MePEO-*b*-PCCL), which were used to incorporate DOX through physical encapsulation or chemical conjugation, respectively (4,8). To provide selective intracellu-

¹ Faculty of Pharmacy and Pharmaceutical Sciences, University of Alberta, Edmonton, Alberta T6G 2N8, Canada.

² Department of Chemical & Materials Engineering, Faculty of Engineering, University of Alberta, Edmonton, AB, Canada.

³ To whom correspondence should be addressed. (e-mail: alavasanifar@pharmacy.ualberta.ca)

lar delivery of DOX in tumor over healthy cells, in this study, the shell of PEO-*b*-P(CL-DOX) and PEO-*b*-PBCL micelles (containing chemically conjugated and physically encapsulated DOX in their core, respectively) was decorated with an internalizing antagonist peptide for $\alpha_v\beta_3$ integrin, i.e., GRGDS. The overexpression of $\alpha_v\beta_3$ integrins on the surface of tumor endothelial cells and metastatic cancer cells has been well documented (9–11). The GRGDS-PEO-*b*-PBCL micellar nanocontainers and GRGDS-PEO-*b*-P(CL-DOX) micellar drug conjugates were hypothesized to act as multifunctional polymeric micelles, where RGD peptide endows micelles preferential entrance to the acidic endosomes of metastatic cancer cells, and the poly(ester) core ensures intra-endosomal pH triggered core degradation and preferential release of DOX or active DOX derivatives in those cells. A similar concept was the basis for the development of multifunctional polymeric micelles composed of folate-PEO-*b*-poly(aspartic acid) conjugated to DOX through acid cleavable hydrazone bonds producing folate-PEO-*b*-P(Asp)-hyd-DOX by Bae et al. (12,13). The higher thermodynamic stability reflected by the lower critical micelle concentration (CMC) of PCL based micelles *versus* P(Asp) micelles (4) as well as acid catalyzed degradability of the poly(ester) core in comparison to more stable poly(amide) core of P(Asp) are the distinguished characteristics of the multifunctional polymeric micelles developed here.

MATERIALS AND METHODS

Materials and Cell Lines

Diisopropyl amine (99%), benzyl chloroformate (tech. 95%), sodium (in Kerosin), butyl lithium (Bu-Li) in hexane (2.5 M solution), 3, 3-diethoxy-1-propanol (DEP), naphthalene, ethylene oxide (EO) and potassium were purchased from Sigma Chemicals (St. Louis, MO, USA). ϵ -caprolactone was purchased from Lancaster Synthesis, UK and distilled by calcium hydride upon use. Stannous octoate was purchased from MP biomedical Inc., Germany. Linear GRGDS was purchased from Bachem (Torrence, CA, USA). Potassium naphthalene solution was prepared by conventional method and the concentration was determined by titration (14). Cell culture media RPMI 1640, penicillin-streptomycin, fetal bovine serum, L-glutamine and HEPES buffer solution (1 M) were purchased from GIBCO, Invitrogen Corp (USA). Doxorubicin (DOX.HCl) was purchased from Hisun Pharmaceutical Co. (Zhejiang, China). All other chemicals were reagent grade. B16F10 Cells were grown as adherent cultures and maintained in RPMI 1640 supplemented with 10% fetal bovine serum at 37°C and 5% CO₂. Acetal-PEO was synthesized by anionic ring-opening polymerization of ethylene oxide at room temperature under argon stream adopting a previously reported method with some modifications (15).

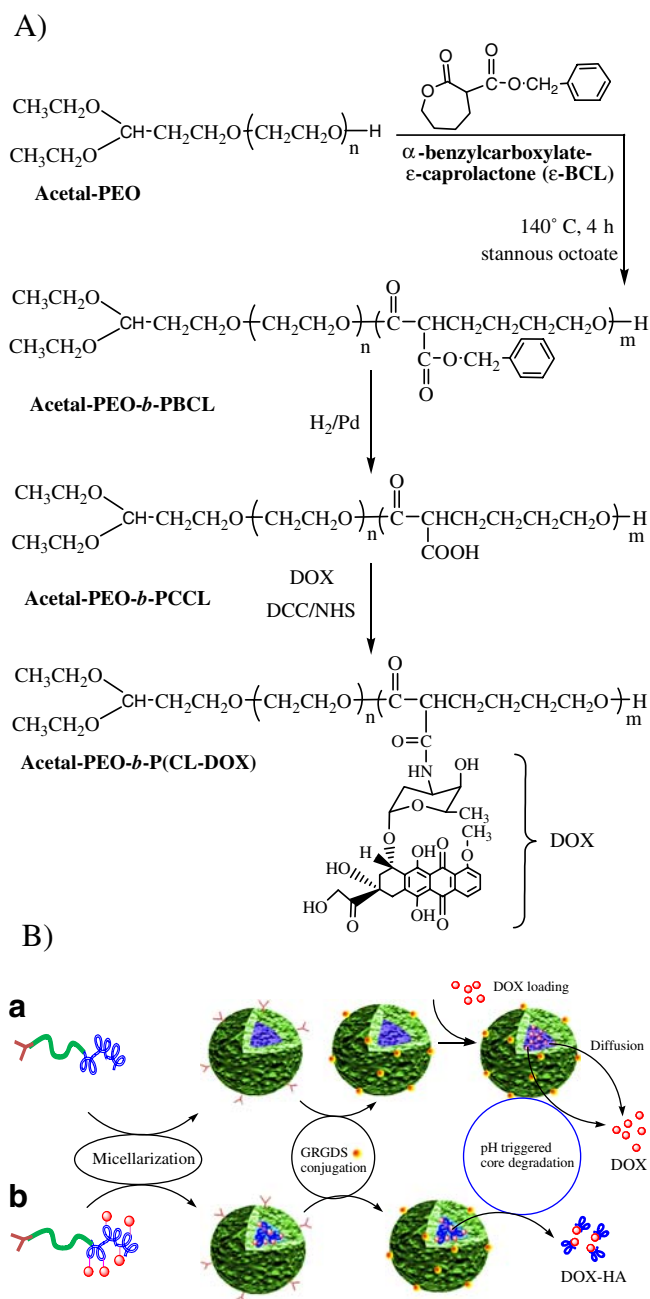
Synthesis of Acetal-PEO-*b*-PBCL Block Copolymer

The functionalized monomer, i.e., α -benzylcarboxylate- ϵ -caprolactone, was synthesized according to the method reported elsewhere (4). Briefly, to a solution of 60.0 mmol (8.4 ml) of dry diisopropylamine in 60 ml of dry THF in a three neck round bottom flask, 60.0 mmol (24 ml) of BuLi in

hexane were slowly added at -30°C under vigorous stirring with continuous argon supply. The solution was cooled to -78°C and kept stirring for additional 20 min. Freshly distilled ϵ -caprolactone (30 mmol or 3.42 g) was dissolved in 8 mL of dry THF and added to the above mentioned mixture slowly, followed by the addition of benzyl chloroformate (30 mmol, 5.1 g). The temperature was allowed to rise to 0°C after 1.5 h and the reaction was quenched with 5 ml of saturated ammonium chloride solution. The reaction mixture was diluted with water and extracted with ethyl acetate (3×40 ml). The combined extracts were dried over Na₂SO₄ and purified by column chromatography using an eluant of 25% EtOAc in hexane. Acetal-PEO-*b*-PBCL was synthesized by ring opening polymerization of α -benzylcarboxylate- ϵ -caprolactone using acetal-PEO as initiator and stannous octoate as catalyst (16). For comparison, acetal-PEO-*b*-PCL was also synthesized using the same method.

Synthesis of Acetal-PEO-*b*-P(CL-DOX) Block Copolymer

Acetal-PEO-*b*-P(CL-DOX) was prepared from acetal-PEO-*b*-PBCL in two steps (Scheme 1A). In the first step, acetal-PEO-*b*-poly(α -carboxyl- ϵ -caprolactone) (acetal-PEO-*b*-PCCL) was obtained by removal of the benzyl groups of acetal-PEO-*b*-PBCL in the presence of H₂. For this purpose, acetal-PEO-*b*-PBCL (1 g) was dissolved in 25 ml of THF and placed into a 100 ml round bottom flask. Then, charcoal-coated with palladium (300 mg) was dispersed in this solution and H₂ was introduced to the reaction flask. After stirring for 24 h in the presence of H₂, the reaction mixture was centrifuged at 3,000 rpm to remove the catalyst. The supernatant was collected, condensed under reduced pressure, precipitated in diethyl ether and washed repeatedly to remove impurities. The final product was dried under vacuum at room temperature for 48 h. In the second step, DOX was conjugated to the acetal-PEO-*b*-PCCL by amide bond formation between the amino group of DOX and the free carboxyl groups on the PCCL chain using N, N-dicyclohexyl carbodiimide (DCC) and N-hydroxysuccinimide (NHS) as the coupling agents. Briefly, to a solution of acetal-PEO-*b*-PCCL (50 mg, ~ 0.01 mmol) in 10 ml of dry THF, DCC and NHS in THF was added, and the reaction mixture was left under constant stirring for 2 h till precipitate was formed. The precipitate was removed by filtration. The solution of DOX.HCl (10 mg, 0.017 mmol) and triethylamine (1.74 mg, 0.017 mmol) in methanol (5 ml) was added drop-wise to the polymer solution. The reaction proceeded for another 24 h under stirring at room temperature. The resulting solution was centrifuged to remove the precipitate followed by evaporation under vacuum to remove the solvents. Methanol (10 ml) was then introduced to dissolve the product. The resulting solution was first purified by Sephadex LH-20 column using methanol as the eluent, and then dialyzed (M_w cut off of 3,500 Da, Spectrum Laboratories, USA) extensively against water to remove free DOX. The resulted polymeric DOX solution was finally freeze-dried for further use. The red powder was dissolved in methanol and evaluated by reversed phase-HPLC (RP-HPLC) to confirm the absence of unbound free DOX. Reversed phase chromatography was carried out with a 10 μm C18–125 Å column (3.9 \times 300 mm, Waters) using a Waters 625 LC system. Twenty microliter of the sample were injected in a gradient elution



Scheme 1. **A** Synthetic scheme for the preparation of acetal-PEO-*b*-PBCL and acetal-PEO-*b*-P(CL-DOX) block copolymers; **B** Models for the preparation and modes of DOX release from *a* GRGDS-PEO-*b*-PBCL/DOX micelles which contain physically encapsulated DOX and *b* GRGDS-PEO-*b*-P(CL-DOX) micelles which contain chemically conjugated DOX.

using 0.05% trifluoroacetic acid aqueous solution and acetonitrile at a flow rate of 1.0 ml/min. The percentage of acetonitrile in the mobile phase was increased from 15% to 85% within 15 min at a constant rate. The detection was performed at 485 nm using a Waters 486 UV/Vis absorbance detector. The degree of DOX conjugation was expressed in mol % with respect to the α -carboxylic- ϵ -caprolactone residue of acetal-PEO-*b*-PCCL, which was estimated from the peak intensity ratio of the aromatic protons (δ 7.35 ppm) of DOX to that of methylene ($-\text{CH}_2\text{O}-$, δ 4.05 ppm) in the PCCL segment of the

block copolymer. The content of conjugated DOX in synthesized polymer, i.e., acetal-PEO-*b*-P(CL-DOX), was determined by measuring its absorbance at 485 nm, on the assumption that molar absorptivity of DOX residue bound to the polymer was identical to that of free DOX at 485 nm.

Preparation of GRGDS-modified Polymeric Micelles

The RGD-peptide was conjugated to the micellar surface by the functional acetal groups on the micellar shell (Scheme 1B). Prepared block copolymers, i.e., acetal-PEO-*b*-PBCL and acetal-PEO-*b*-P(CL-DOX), were assembled to polymeric micelles by dissolving the polymers (20 mg) in acetone (1 mL) and drop-wise addition (\sim 1 drop/15 s) of polymer solutions to doubly distilled water (6 ml) under moderate stirring at 25°C, followed by the evaporation of acetone under vacuum. The aqueous solution of polymeric micelles was then acidified to pH 2.0 with diluted HCl (0.5 mol/l) and kept stirring for 2 h at room temperature to produce aldehyde-polymeric micelles. The resulted solution was then neutralized with NaOH (0.5 mol/l). The micellar solution was extensively dialyzed (M_w cut-off 3,500) against water to remove the salt, concentrated by ultrafiltration with MILLIPORE Centrifugal Filter Device (M_w cut-off 100,000 Da), and freeze-dried. The dry powder was then dissolved in CDCl_3 (40 mg/ml) for ^1H NMR analysis. For GRGDS conjugation, the micellar aqueous solution was concentrated followed by the addition of an appropriate volume of concentrated sodium phosphate buffer solution to obtain a 4 mg/ml polymer concentration (pH=7.0, ionic strength 0.1 M). GRGDS was added and incubated with aldehyde-PEO-*b*-PBCL and aldehyde-PEO-*b*-P(CL-DOX) micelles at GRGDS:polymer molar ratio of 1:2 at room temperature for 2 h under moderate stirring. Subsequently, NaBH_3CN (10 eq.) was added to the polymer to reduce the Schiff base. After 90 h of reaction, unreacted peptide and reducing reagent were removed by extensive dialysis against water. The conjugation efficiency of GRGDS to polymeric micelles was assessed by a gradient reverse HPLC method as previously reported (17).

Characterization of Prepared Block Copolymers and Polymeric Micelles

Synthesized copolymers were analyzed by gel permeation chromatography (GPC) and ^1H NMR. GPC was carried out at 25°C with an HP instrument equipped with Waters Styragel HT4 column (Waters Inc., Milford, MA, USA). The elution pattern was detected at 35°C by refractive index (PD2000, Percision Detectors, Inc.) and light scattering detectors (Model 410, Waters Inc). THF was used as eluent at a flow rate of 1.0 ml/min. ^1H NMR spectra were measured by a Bruker Unity-300 ^1H NMR spectrometer at room temperature, using CDCl_3 or $\text{DMSO}-d_6$ as solvent and tetramethylsilane as internal reference.

Average diameter and size distribution of prepared micelles were estimated by dynamic light scattering (DLS) using Malvern Zetasizer 3000 at a polymer concentration of 4 mg/ml in water at 25°C after filtration through 0.45 μm filters (Fisher Scientific, USA). A change in the fluorescence excitation spectra of pyrene in the presence of varied

concentrations of block copolymers was used to measure their CMC (18). The viscosity of micellar cores was estimated by measuring excimer to monomer related peaks (at 373 and 480 nm, respectively) intensity ratios (I_e/I_m) from the emission spectra of 1,3-(1,1'-dipyrenyl)propane (18).

Physical Encapsulation of DOX in Acetal- and GRGDS-PEO-*b*-PBCL Micelles

Acetal- or GRGDS-PEO-*b*-PBCL (10 mg) and DOX (2 mg) were dissolved in acetone (2 ml) in a glass vial followed by the addition of 3.0 equivalent of triethylamine (TEA). This solution was added drop-wise to distilled water (12 ml) under moderate stirring at 25°C. The glycosidic amino group in DOX was deprotonated in the presence of TEA. The micellar solution was then left stirring overnight, allowing slow evaporation of acetone. Vacuum was then applied to ensure the removal of residual acetone. DOX-loaded polymeric micellar solutions were then dialyzed against a large quantity of water for 8 h using a pre-swollen semi-permeable membrane (Spectra/Pro 6, M_w cut-off 3,000, Spectrum, Houston, USA) to remove unloaded DOX. Average diameter and size distribution of prepared micelles were estimated by DLS. The extent of DOX encapsulation in micelles (wt%) was quantified photometrically at 485 nm after redissolving the freeze-dried sample in a DMSO-CHCl₃ mixture (1:1, *v/v*). The extent of DOX incorporation in polymeric micelles in terms of weight and molar percent of DOX to polymer was calculated based on the following equations:

$$\text{weight \% (drug/polymer)} = \frac{\text{amount of loaded DOX in mg}}{\text{amount of copolymer in mg}} \times 100 \%$$

$$\text{molar \% (drug/polymer)} = \frac{\text{Molecular weight of polymer}}{\text{Molecular weight of DOX}} \times \text{weight \% (drug/polymer)}$$

Drug Release from DOX Loaded Micelles

The *in vitro* release from micelles was investigated by dialysis method. The dialysis was conducted in Dulbecco's phosphate buffered saline (PBS, pH 7.2), 0.1 M acetate buffer (pH 5.0) or 10% fetal bovine serum in PBS (pH 7.2). Micellar solution containing physically encapsulated DOX or chemically conjugated DOX diluted in the media at initial concentration of 300–400 µg/ml was placed in a dialysis bag (M_w cut-off: 3,000 g mol⁻¹, Spectrum Laboratories, USA). The dialysis bag was immersed in the media at 37°C at ten times volume of micellar solution inside the dialysis bag. At certain time intervals, micellar solution in the dialysis bag was sampled, dissolved in DMSO, centrifuged and subjected to photometrical assay at 485 nm to determine the residual DOX content. To calculate the amount of released drug, DOX remained in the dialysis bag was subtracted from the initial DOX amount used in the release experiment.

Assessing the Degradation Rate of Poly(ester) Core in Acidic and Physiological pH

Acetal-PEO-*b*-P(CL-DOX) and acetal-PEO-*b*-PBCL copolymers were incubated in acetate buffer (pH 5.0) at a

polymer concentration of 1 mg/ml (above CMC). At different time points, 5 ml of incubation medium was withdrawn and extensively dialyzed against water to remove all possible degradation products. The remaining polymer in the dialysis bag was lyophilized, and redissolved in CDCl₃ for calculation of block copolymer M_n by ¹H NMR analysis. The percentage of poly(ester) block remained in the copolymers of acetal-PEO-*b*-PBCL or acetal-PEO-*b*-P(CL-DOX) at different degradation time points was estimated from the following equation:

$$\text{Remained poly(ester)\%} = \frac{M_n \text{ of block copolymer after hydrolysis} - M_n \text{ of PEO}}{M_n \text{ of block copolymer before hydrolysis} - M_n \text{ of PEO}} \times 100 \%$$

At the end point of the study (144 h), micellar solution was lyophilized to a dry powder, redissolved in 1 ml THF, passed through a 0.4 µm syringe filter and analyzed by GPC as described under polymer characterization. The fractions generated from GPC column after injection of block copolymer samples of acetal-PEO-*b*-P(CL-DOX) incubated in pH 5.0 for 144 hs were collected and analyzed by LC/MS (Waters Micromass ZQ 4000, MA, USA). The latter experiment was carried out on acetal-PEO-*b*-P(CL-DOX) and acetal-PEO-*b*-PBCL incubated in PBS (pH 7.4) for 144 h, as well.

Cellular Uptake of Polymeric Micelles by B16F10 Cells

Flow cytometry studies were conducted to determine the association of DOX incorporated polymeric micelles by B16F10 cells. Cells grown in the six-well plate as a monolayer were incubated with free DOX, GRGDS- and acetal- micelles of PEO-*b*-P(CL-DOX) or PEO-*b*-PBCL containing chemically or physically incorporated DOX (5 µg equivalent DOX/mL), respectively, for 4 h at 37°C. Single cell suspension were prepared by brief treatment with trypsin, washed with PBS, filtered through 35 µm nylon mesh, and finally examined on a FACsort™ flow cytometer (Becton-Dickinson Instruments, Franklin Lakes, NJ, USA). Ten thousand cells were counted with logarithmic settings. The cell-associated DOX was excited with an argon laser (488 nm) and the fluorescence was detected at 560 nm.

Confocal fluorescent microscopy was used to compare the intracellular uptake of DOX from GRGDS- or acetal-PEO-*b*-P(CL-DOX) and GRGDS- or acetal-PEO-*b*-PBCL micelles containing physically encapsulated DOX. The intracellular disposition of polymeric micelles in B16F10 cells was also evaluated. B16F10 cells were grown on coverslips to 50% confluence and incubated with free DOX and micelles containing chemically or physically loaded DOX (5 µg equivalent DOX/ml) diluted in culture medium at 37°C for 4 h, separately. Cells were incubated with LysoTracker blue DND-22 (50 nM, Molecular Probe, OR, USA) for 2 h for endosome/lysosome labelling. The cells were then washed three times with PBS, fixed in paraformaldehyde in PBS for 10 min. For nucleus labelling, fixed cells were washed with PBS and then incubated with DAPI (Molecular Probes) for 15 min. In the competition test, B16F10 cells were first incubated with excess of free GRGDS (2 mM) for 30 min and

then incubated with GRGDS-modified DOX incorporated micelles. Cells were examined by a confocal microscope (Zeiss 510 LSMNLO, Jena, Germany). The excitation and emission wavelengths were set at 480 and 540 nm, respectively.

In vitro Cytotoxicity Study

Cytotoxicity of chemically conjugated or physically encapsulated DOX in acetal and GRGDS-micelles against B16F10 cells was evaluated using 3-(4,5-dimethylthiazol-2-yl)-2,5-diphenyltetrazolium bromide (MTT) assay. Growth medium RPMI-1640 (100 μ l) containing 4,000 cells was placed in each well in 96-well plates and incubated overnight to allow cell attachment. Cells were then exposed to serial dilutions of different formulations at 37°C for 24 or 48 h, followed by the addition of 20 μ l of MTT solution. Three hours later, medium was aspirated and the precipitated formazan was dissolved in 200 μ l of DMSO. Cell viability was determined by measuring the optical absorbance differences between 570 and 650 nm using a PowerwaveX340 microplate reader (BIO-TEK Instruments, Inc., Nepean, Ontario, Canada). The mean and standard deviation of cell viability for each treatment was determined, converted to the percentage of viable cells relative to the control. The concentration of drugs required for 50% growth inhibition (IC_{50} values) was estimated from a plot of the percentage of viable cells *versus* log DOX concentration for each treatment.

Statistical Analysis

Values are presented as mean \pm standard deviation (SD) of triple measurements. Statistical significance of differences was tested using either unpaired Students' *t* test or one-way ANOVA test (SSPS for Windows v.13, Cary, NC, USA). Differences between means of IC_{50} were assessed using One way ANOVA followed by *post hoc* analysis using Dunnett T3 test. The level of significance was set at $\alpha=0.05$.

RESULTS

Preparation and Characterization of Block Copolymers

The 1H NMR spectra of starting and intermediate polymers in the synthetic process are shown in Fig. 1. In the 1H NMR spectrum of acetal-PEO-*b*-PBCL in $CDCl_3$, peaks appeared at δ 1.20 (t), 1.25–2.00 (m), 3.65 (s), 4.05 (t), 4.65 (t), 5.15 (s), 7.35 (s). The yield for the production of acetal-PEO-*b*-PBCL from polymerization of α -benzylcarboxylate- ϵ -caprolactone with acetal-PEO was 92.4%. 1H NMR spectrum of reduced block copolymer, acetal-PEO-*b*-PCCL, in $CDCl_3$ revealed existence of peaks at δ 1.20 (t), 1.25–2.00 (m), 3.65 (s), 4.05 (t), 4.65 (t) and absence of the characteristic benzyl peak at δ 7.35 ppm. The yield for the preparation of acetal-PEO-*b*-PCCL block copolymer from acetal-PEO-*b*-PBCL was 80.0%. The 1H NMR of acetal-PEO-*b*-P(CL-DOX) in $DMSO-d_6$, on the other hand, produced peaks at δ 1.20 (t), 1.25–2.0 (m), 3.65 (s), 4.05 (t), 4.55 (t), 5.60 (d), 7.35 (s) and the yield for the production of acetal-PEO-*b*-P(CL-DOX) from acetal-PEO-*b*-PCCL was 73%.

The measured molecular weight of P(CL-DOX) (M_n \sim 1,800 $g\ mol^{-1}$) is lower than the expected P(CL-DOX)

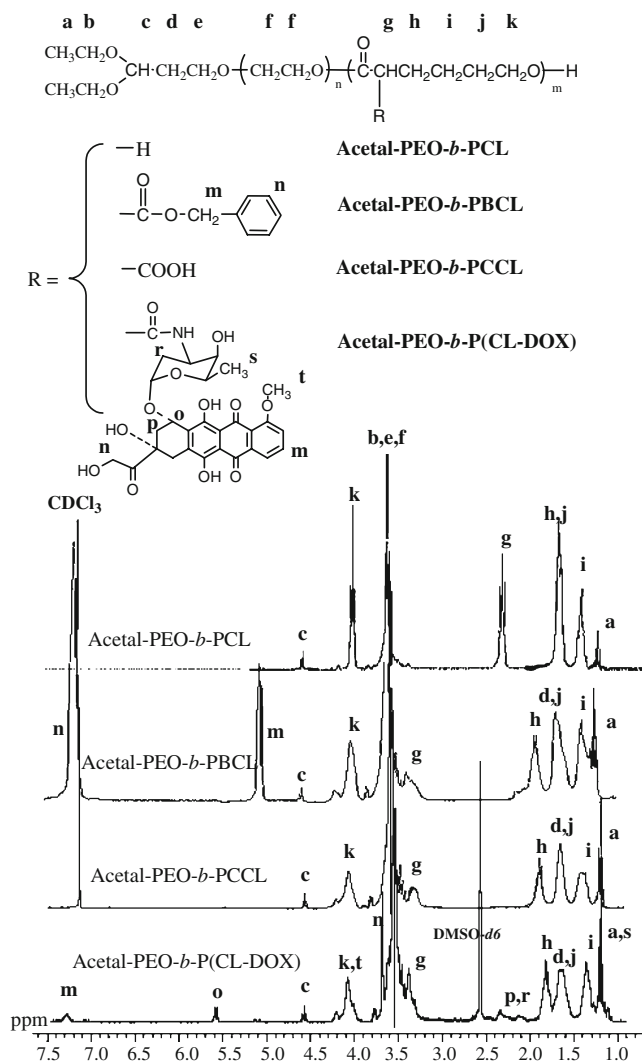


Fig. 1. 1H NMR spectra of acetal-PEO-*b*-PCL, acetal-PEO-*b*-PBCL, acetal-PEO-*b*-PCCL in $CDCl_3$, and acetal-PEO-*b*-P(CL-DOX) in $DMSO-d_6$.

molecular weight ($2,670\ g\ mol^{-1}$), suggesting incomplete substitution of DOX or possible chain cleavage of poly (ester) block during conjugation process. The degree of DOX conjugation on the block copolymer was 11.1% (molar ratio of DOX to CL unit) as estimated by comparing the peak intensity of DOX (δ 7.35) to that of PCL-DOX (δ 4.05) in its 1H NMR spectrum in $DMSO-d_6$.

Prepared block copolymers self assembled to micelles and treated with acid so that the acetal groups on the micellar surface were converted to functional aldehyde groups for RGD peptide conjugation (Scheme 1B). In the 1H NMR spectra of the acid treated polymers, the peaks corresponding to the acetal group (methyl protons of CH_3CH_2O , δ 1.2 ppm and methylene protons of $OCHCH_2$, δ 4.6 ppm) disappeared and the related peak for the aldehyde proton appeared at δ 9.8 ppm. Measurements by GPC revealed M_n values of 5,100, 4,020 and 5,200 $g\ mol^{-1}$ for aldehyde-PEO-*b*-PBCL, aldehyde-PEO-*b*-PCCL and aldehyde-PEO-*b*-P(CL-DOX) block copolymers, respectively. The polydispersities of block copolymers were 1.74, 1.40 and 1.37, respectively. The similarity between the molecular weight and polydispersity

of aldehyde- and acetal-polymers suggests limited chain cleavage in the poly(ester) block during 2 h incubation at pH 2.0. Measurement of the concentration of free GRGDS remaining after 96 h reaction by HPLC revealed a conjugated GRGDS/polymer molar ratio of 1:2 at a molar peptide/polymer feed ratio of 1:2, corresponding to 100% conjugation efficiency.

Preparation and Characterization of Polymeric Micelles

The results of characterization studies on acetal- and GRGDS-modified PEO-*b*-PBCL and PEO-*b*-P(CL-DOX) micelles with respect to their CMC, particle size, and core viscosity are summarized in Table I. In comparison to acetal-PEO-*b*-PCL, introduction of hydrophobic benzyl groups resulted in copolymer acetal-PEO-*b*-PBCL with a lower CMC, revealing a better thermodynamic stability for the latter structure. DOX-conjugated copolymers showed significantly higher CMC than PEO-*b*-PCL and PEO-*b*-PBCL due to the introduction of more hydrophilic DOX and existence of free carboxyl groups in the core-forming block. Polymeric micelles under the study showed rigid cores as evidenced by a low intensity of the excimer peak in the fluorescence emission spectra of 1,3-(1,1'-dipyrenyl) propane in the presence of block copolymers at concentrations above their CMC (~ 1 mg/ml). Micellar cores consisting of PBCL and PCL were found to be more rigid than P(CL-DOX) cores. GRGDS-attached polymers displayed similar CMC and I_e/I_m to their acetal-counterparts, indicating the independence of core properties from shell modification in the polymeric micellar structure. The average diameter of micelles under current study was between 48–92 nm and they illustrated no sign of aggregation within one month of storage at 4°C.

The characteristics of DOX incorporated acetal- and GRGDS-micelles are shown in Table II. No significant difference in the level of DOX incorporation between GRGDS- and acetal-PEO-*b*-PBCL micelles was observed pointing to the incorporation of DOX in the PBCL core. Average diameter of acetal- or GRGDS-PEO-*b*-PBCL micelles containing physically encapsulated DOX was lower than acetal- and GRGDS-PEO-*b*-P(CL-DOX) micelles. All the prepared micellar solutions with physically loaded or chemically conjugated DOX demonstrated good stability and no sign of aggregation or precipitation within one month of storage at 4°C.

In vitro DOX Release and Hydrolytic Degradation of the Micellar Core in Acidic and Physiological pH

Physically encapsulated DOX was released from polymeric micelles in a typical two phase profile showing burst release at initial time points and more sustained release after 6 h incubation in pH 7.2 (Fig. 2A). DOX release from PBCL containing polymeric micelles was found to be significantly higher at pH 5.0 compared to pH 7.2 for all time points within 72 h experiment. DOX release from PBCL core was slightly but not significantly increased in the presence of 10% serum ($P > 0.05$). No significant difference was observed between DOX releases from acetal- and GRGDS-PEO-*b*-PBCL micelles at pH 7.2. DOX-conjugated micelles didn't show detectable DOX release in the used media based on spectrophotometrical assay.

Table I. Characteristics of the Polymer and Prepared Polymeric Micelles ($n=3$)

Polymer ^d	Polymer M_n^b (g mol ⁻¹)	Polymer M_n^c (g mol ⁻¹)	Polydispersity ^e (M_w/M_n)	CMC ^d \pm SD (μ M)	$I_e/I_m \pm$ SD	Average diameter ^f (nm)	PDI ^{f, g}
Acetal-PEO ₈₂ - <i>b</i> -PCL ₂₈	6,820	6,430	1.27	0.59 \pm 0.06	0.35 \pm 0.01	93.0 \pm 4.0	0.22
Acetal-PEO ₈₂ - <i>b</i> -PBCL ₁₂	6,660	5,240	1.64	0.39 \pm 0.05****	0.29 \pm 0.01****	69.1 \pm 3.4**	0.27
GRGDS-PEO ₈₂ - <i>b</i> -PBCL ₁₂	6,670	4,980	1.46	0.38 \pm 0.03****	0.28 \pm 0.01****	72.3 \pm 2.5**	0.31
Acetal-PEO ₈₂ - <i>b</i> -P(CL-DOX) ₁₀	5,450	5,130	1.41	4.95 \pm 0.22****	0.41 \pm 0.03****	89.4 \pm 2.9	0.18
GRGDS-PEO ₈₂ - <i>b</i> -P(CL-DOX) ₁₀	5,360	5,250	1.35	4.91 \pm 0.19****	0.40 \pm 0.06****	91.6 \pm 3.5	0.21

^a The M_w of PEO was 3,600 g mol⁻¹ based on GPC analysis; the subscript numbers represent the polymerization degree of each block based on ¹H NMR analysis

^b Determined by ¹H NMR

^c Determined by GPC

^d Measured from the onset of a rise in the intensity ratio of peaks at 339 nm to peaks at 334 nm in the fluorescence excitation spectra of pyrene plotted versus logarithm of polymer concentration;

^e Intensity ratio (excimer/monomer) from emission spectrum of 1,3-(1,1'-dipyrenyl) propane in presence of polymeric micelle

^f Estimated by DLS technique

^g Polydispersity index (PDI)

** $p < 0.05$, when compared to their DOX-conjugated counterparts

*** $p < 0.01$, when compared to their DOX-conjugated counterparts

**** $p < 0.05$ when compared to acetal-PEO-*b*-PCL

Table II. Characteristics of the Polymeric Micelles Containing Physically Loaded and/or Chemically Conjugated DOX ($n=3$)

DOX-loaded micelles	Average diameter (nm) ^a	PDI ^{a, b}	DOX incorporation	
			drug/polymer (wt%)	drug/polymer (molar%)
Acetal-PEO- <i>b</i> -PBCL/DOX	68.4±2.4*	0.28	3.78±0.05	46.36±0.61
GRGDS-PEO- <i>b</i> -PBCL/DOX	69.6±3.2**	0.19	3.62±0.14	44.47±1.70
Acetal-PEO- <i>b</i> -P(CL-DOX)	89.4±2.9	0.18	3.64±0.04	36.53±0.40
GRGDS-PEO- <i>b</i> -P(CL-DOX)	91.6±3.5	0.21	3.58±0.06	35.34±0.60

^a Estimated by DLS technique^b Polydispersity index (PDI)^c estimated by UV/Vis method* $p < 0.01$, when compared to acetal-PEO-*b*-P(CL-DOX)** $p < 0.01$, when compared to GRGDS-PEO-*b*-P(CL-DOX)

Instead, under acidic or enzymatic environment such as in endosome, the poly(ester) block of the copolymer can be degraded by hydrolysis and DOX derivative would be released as suggested in Scheme 1B. GPC and ¹H NMR were used to confirm the core degradation. The molecular weight loss of PBCL and P(CL-DOX) based on ¹H NMR analysis during acidic hydrolysis are shown in Fig. 2B. ¹H NMR analysis revealed a decrease in the M_n of polyester block as a result of incubation of P(CL-DOX) and PBCL core-containing micelles in acetate buffer (pH 5.0), pointing to the degradation of the poly(ester) core. The degradation of P(CL-DOX) core was much faster than that of PBCL core in corresponding polymeric micelles. A 40% decrease in the M_n of acetal-PEO-*b*-P(CL-DOX) (from 1,850 to 1,200) was observed compared to the <10% decrease in the M_n of acetal-PEO-*b*-PBCL (from 3,600 to 3,200) for after 144 h incubation. The hydrolytic products from acetal-PEO-*b*-PBCL and acetal-PEO-*b*-P(CL-DOX) after 144 h of incubation were further analyzed by GPC (Fig. 2C, D) and LC/MS. Incubation of acetal-PEO-*b*-P(CL-DOX) micelles in pH 5.0 after 144 h produced a new predominant peak with an increased retention time (11.03 min) compared to the original polymer (Fig. 2C). Further analysis of the new peak by LC/MS revealed the presence of compounds with molecular weights of 701.28 and 176.17 g mol⁻¹, which matches the molecular weights of the expected degradation products from P(CL-DOX), i.e., 2-DOX-6-hydroxyhexanoic acid (DOX-HA) and 2-(4-hydroxybutyl)malonic acid (HBMA), respectively (data not shown). The GPC chromatogram of acetal-PEO-*b*-PBCL after incubation also revealed an increase in the retention time for the polymer and a relatively weaker new peak at ~11.08 min (Fig. 2D), which can be attributed to the degradation products such as 2-(benzyloxy)carbonyl-6-hydroxyhexanoic acid or HBMA. In contrast, no noticeable degradation was observed after incubation of acetal-PEO-*b*-P(CL-DOX) and acetal-PEO-*b*-PBCL micelles at pH 7.2 for 144 h (inserted panel in Fig. 2C and D, respectively).

Cellular Uptake and Localization of Acetal- and GRGDS-polymeric Micellar DOX in B16F10 Cells

The cellular uptake of DOX from different formulations was studied by flow cytometry (Fig. 3A). As expected, the highest amount of cell-associated fluorescence was observed with free DOX. Decoration of polymeric micellar surface with GRGDS increased the cellular uptake of micelles

containing physically incorporated DOX (Fig. 3A-a) or conjugated DOX (Fig. 3A-b) by B16F10 cells. Micelles of GRGDS-PEO-*b*-PBCL containing physically encapsulated DOX provided slightly higher DOX intracellular concentrations than GRGDS-PEO-*b*-P(CL-DOX) micelles containing chemically conjugated DOX.

The cellular uptake was further studied by confocal microscopy (Fig. 3B). Significant increase in the intracellular DOX fluorescent intensity was observed with GRGDS-modified micelles containing chemically or physically incorporated DOX (Fig. 3B-a and c, respectively) compared to their non-RGD counterparts (Fig. 3B-b and d). In the presence of blocking ligand for competition experiment, the cellular uptake of DOX from GRGDS-modified micelles containing chemically or physically loaded DOX was dramatically reduced and became essentially equivalent to that of the unmodified micelles (data not shown), pointing to the involvement of receptor mediated endocytosis in the uptake of GRGDS modified micelles. In contrast to the predominant accumulation of free DOX in the nuclei (Fig. 3B-e), DOX fluorescence for DOX-chemically conjugated micelles was mainly located in the cytoplasm (Fig. 3B-a and b). For physically encapsulated DOX in PBCL based micelles, DOX fluorescence was observed in cytoplasm as well as in the nuclei (Fig. 3B-c and d). The endocytosis of GRGDS-modified micelles by B16F10 cells was demonstrated by LysoTracker staining (Fig. 4). The superimposed images following the co-localization of LysoTracker and DOX incorporated micelles (Fig. 4a and b) but not free DOX (Fig. 4c) showed pink spots in cytoplasm, indicating that GRGDS-attached DOX-loaded micelles were taken up from the extracellular fluid into the cells by endocytosis and entrapped in endosomes/lysosomes compartments of the cells (17,19,20).

In Vitro Cytotoxicity of DOX against B16F10 Cells

Overall, free DOX was shown to be more effective as indicated by the lower IC₅₀ values (0.32 and 0.023 μM for 24 and 48 h incubation, respectively) than the polymeric micellar formulations (IC₅₀ values ranged from 1.22–6.45 and 0.315–1.36 μM after 24 and 48 h incubation, respectively) (Fig. 5). In general, chemically conjugated DOX was found less cytotoxic than physically encapsulated DOX. Modification of the micelles with GRGDS resulted in improved efficacy for both chemically conjugated and physically loaded DOX in polymeric micelles. GRGDS modification of PEO-*b*-PBCL

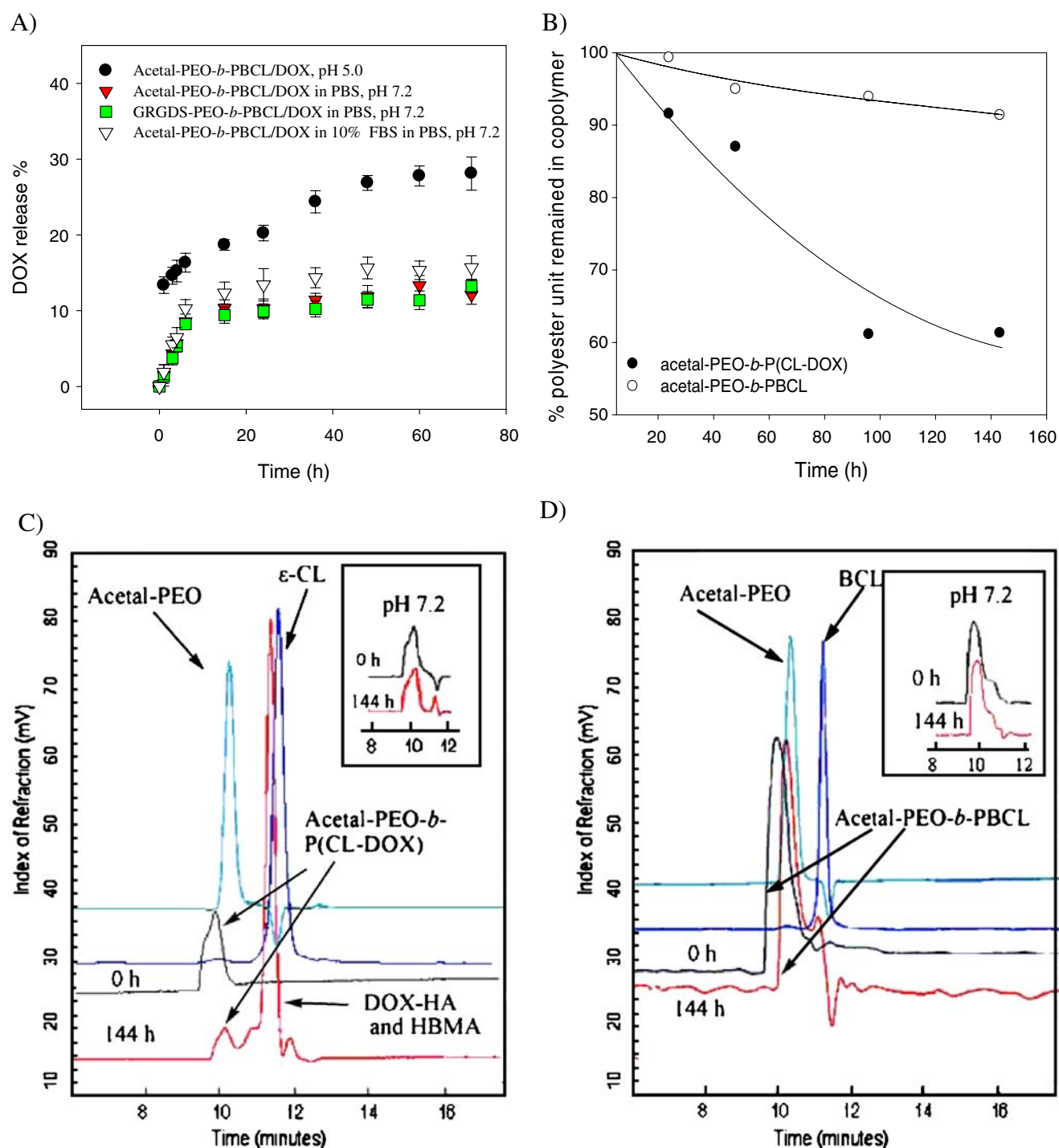


Fig. 2. Acid-catalyzed hydrolysis of poly(ester) core resulted in drug release from micelles with PBCL core and P(CL-DOX) core. **A** Drug release from DOX physically loaded micelles at pH 5.0 and pH 7.2 with or without 10% serum. Acetal-PEO-*b*-P(CL-DOX) micelles didn't show detectable drug release. Each point represents the average of three experiments \pm SD. **B** The rate of poly(ester) core degradation in acetate buffer (pH 5.0) based on ^1H NMR analysis. **C** and **D** GPC analysis of acetal-PEO-*b*-P(CL-DOX) and acetal-PEO-*b*-PBCL block copolymers after 144 h of degradation in acetate buffer (pH 5.0), respectively. The *inserted panel* shows the GPC plot of corresponded copolymers after 144 h of incubation in PBS (pH 7.2).

micelles led to 2.6 and 2.0 fold decrease in the average IC_{50} of physically encapsulated DOX after 24 and 48 h incubation, respectively. For chemically conjugated DOX, 1.9 and 2.7 fold decreases in the average IC_{50} of DOX was observed as a result of micellar surface modification with GRGDS after 24

and 48 h incubation, respectively. In addition, free DOX plus empty acetal-PEO-*b*-PBCL or GRGDS-PEO-*b*-PBCL micelles demonstrated comparable IC_{50} to that of free DOX alone, suggesting these carriers themselves didn't cause extra cytotoxicity to B16F10 cells.

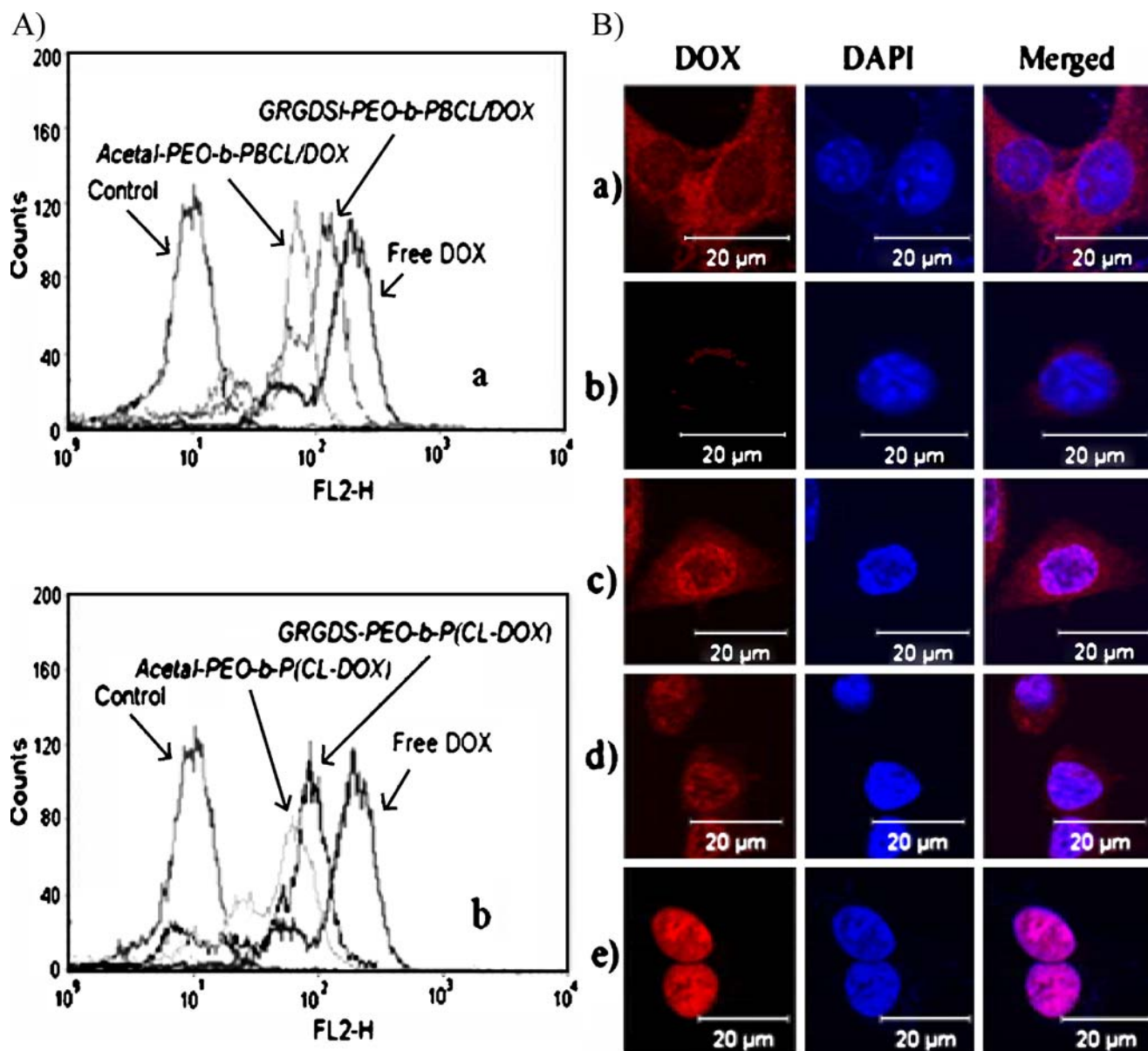


Fig. 3. Cellular uptake of DOX formulated in micelles. **A** Flow cytometry showed enhanced association of GRGDS-modified micelles containing *a* physically loaded DOX and *b* chemically conjugated DOX, with B16F10 cells in comparison to acetal micelles after 4 h incubation at 37°C. Untreated cells served as negative control while free DOX solution was used as positive control. **B** Confocal fluorescent microscopy showed enhanced intracellular uptake and nuclear localization of *a* GRGDS-PEO-*b*-P(CL-DOX) compared to *b* acetal-PEO-*b*-P(CL-DOX); and *c* GRGDS-PEO-*b*-PBCL/DOX micelles compared to *d* acetal-PEO-*b*-PBCL/DOX micelles. Free DOX (*e*) was used as control. Cells were incubated with DOX formulations (5 μ g eq. DOX/ml) for 4 h, washed, fixed in 95% ethanol. Red Doxorubicin fluorescence; blue DAPI fluorescence. A comparison between chemically conjugated DOX and physically encapsulated DOX (*a* versus *c* and *b* versus *d*) points to enhanced nuclear localization of physically encapsulated DOX in comparison to chemically conjugated DOX.

DISCUSSION

The objective of this study was to assess the feasibility of multifunctional polymeric micelles containing acid cleavable poly(ester) based core structures and, at the same time, decorated with RGD ligands on their surface for enhanced anticancer drug delivery to metastatic cancer cells. This specific design was hypothesized to enhance the selective delivery of incorporated anticancer drug (DOX) to metastatic tumor cells through integration of two targeting strategies: (1) First, active targeting of RGD modified carrier to the endosome of metastatic tumor cells that overexpress RGD receptor, i.e., $\alpha_v\beta_3$ integrins; (2) prefer-

ential micellar core degradation and enhanced release of drug or active drug derivatives, exclusively, in the endosomal pH of cells overexpressing $\alpha_v\beta_3$ integrins. Having this general goal in mind, PEO-*b*-PBCL and PEO-*b*-P(CL-DOX) micelles containing physically encapsulated and chemically conjugated DOX in their poly(ester) core and modified on the surface with a model internalizing RGD peptide, i.e., GRGDS were prepared (Scheme 1). The potential of this architecture in providing preferential drug release inside metastatic melanoma B16 cells through combination of aforementioned targeting strategies was investigated. Due to their excellent biodegradability and biocompatibility, PEO-*b*-polyesters represent one of

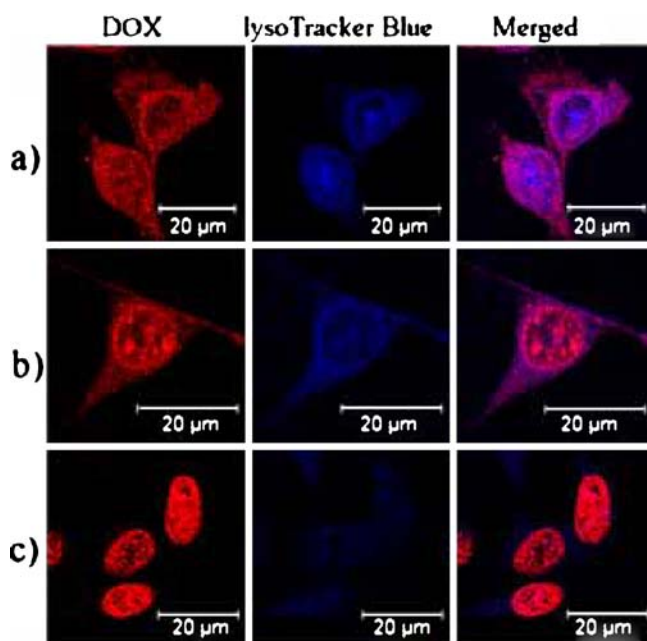


Fig. 4. Confocal fluorescent microscopy showed lysosomal/endosomal localization of **a** GRGDS-PEO-*b*-P(CL-DOX) micelles and **b** GRGDS-PEO-*b*-PBCL/DOX micelles, compared to **c** free DOX. Cells were incubated with DOX formulations (5 $\mu\text{g eq DOX/ml}$) for 4 h, washed, fixed in 95% ethanol. Red Doxorubicin fluorescence; blue LysoTracker blue fluorescence.

the most promising amphiphilic copolymers for micellar self-assembly in drug delivery. Research on cancer-targeted polymeric micelles has been greatly advanced in the past decade (7). However, the potential for simultaneous modification of the PEO block and polyester block and the application of multifunctional PEO-*b*-poly(ester) based micelles for cancer targeting has not been explored sufficiently. To the best of our knowledge, this is the first report on the successful preparation of PEO-*b*-polyester micelles simultaneously bearing functional groups on the PEO shell and several reactive side groups on the polyester core and their application as multifunctional polymeric micelles with controlled core degradation and drug release properties for anticancer drug targeting.

Successful synthesis of GRGDS decorated PEO-*b*-PBCL and PEO-*b*-P(CL-DOX) copolymers provided evidence for the feasibility of acetal installation on the PEO end and Schiff base chemistry in the preparation of multifunctionalized PEO-*b*-poly(ester) based copolymers. This synthetic approach has previously been utilized to modify the surface of conventional PEO-*b*-poly(ester) micelles such as PEO-*b*-poly(D, L-lactide) and PEO-*b*-PCL micelles (17,21). Scission of the polyester core could happen but would be minimized since the hydrophobic micellar core is segregated from the aqueous environment during conversion of acetal-ended micelles to aldehyde-ended micelles under treatment of pH 2.0 for 2 h. However, due to the relatively more hydrophilic core of P(CL-DOX) compared to PBCL core, a drop in the molecular weight was observed for P(CL-DOX) core (from 1,850 to 1,700 $\text{g}\cdot\text{mol}^{-1}$) but not for PBCL core (from 3,060 to 3,040 $\text{g}\cdot\text{mol}^{-1}$), which is consistent with the results of core degradation under pH 5.0 (Fig. 2B).

The first part of our assessments on this system provided evidence for preferential degradation of the poly(ester) core

and DOX release in endosomal pH from both PBCL and P(CL-DOX) related systems. The results of studies on the rate of PBCL and P(CL-DOX) core degradation in acidic environments mimicking the pH of endosomal/lysosomal organelles provided evidence for acid catalyzed hydrolysis of the poly(ester) core as suggested in Scheme 1B. Overall, in comparison to PBCL, the P(CL-DOX) core was more stable in neutral pH to avoid premature drug release, and more susceptible to degradation specially in pHs that mimic endosomal pH (Fig. 2A–D). This might be related to the higher hydrophobicity and rigidity of PBCL in comparison to P(CL-DOX) cores, as evidenced by lower CMC and I_e/I_m ratios, respectively (Table I), which restricts the movement of water required for hydrolysis of the poly(ester) core (22).

Release of physically encapsulated DOX from its carrier is dependent on both the rate of drug diffusion from micellar core and core degradation; whereas for conjugated DOX, core degradation plays a major role in drug release. We observed a significant release of physically encapsulated DOX in both physiological and endosomal pHs but not for DOX conjugated micelles (Fig. 2A). Release of physically encapsulated DOX was higher in pH 5.0, possibly due to the higher water solubility of protonated DOX molecule in this pH, which drives DOX diffusion and release out of its carrier. A preferential degradation of PBCL core in acidic pH might have accelerated DOX release from the PBCL core after 24 h incubation time point leading to a three phasic release profile for this structure (Fig. 2A). In contrast to physically encapsulated DOX, no loss of chemically conjugated DOX from its carrier was detected during the dialysis study in pH 5.0. The observation may reflect production of DOX derivatives with either molecular weights larger than the molecular weight cut-off of the dialysis membrane or very low water solubility (e.g., DOX-HA) disrupting sink conditions in the release experiment. Noticeably, both the drug release and degradation data showed that DOX conjugated micelles are more stable at pH 7.2 compared to DOX physically loaded micelles (Fig. 2A, C), therefore a greater change in the pharmacokinetics and tumor-targeted delivery of DOX after

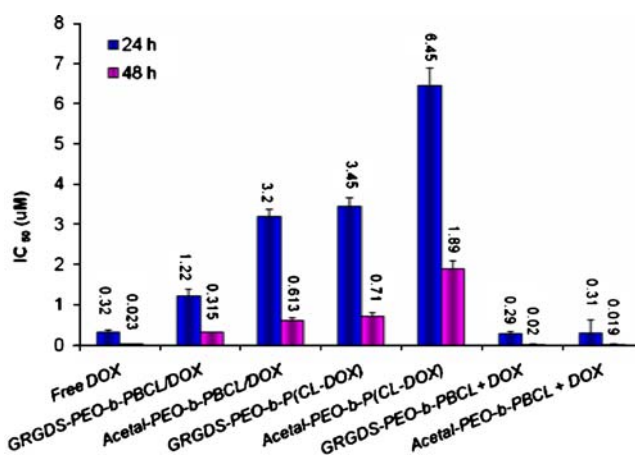


Fig. 5. Cytotoxicity of various DOX formulations against B16-F10 cells by MTT assay. Each bar represents the average IC₅₀ value of DOX, estimated from a plot of the percentage of viable cells versus log DOX concentration, from three independent experiments \pm SD.

systemic administration of GRGDS-PEO-*b*-P(CL-DOX) conjugates compared to physically encapsulated DOX in GRGDS-PEO-*b*-PBCL micelles is envisioned (23).

In the second part, the experiments were designed to investigate the potential benefit of RGD modification of PEO-*b*-poly(ester) micelles for DOX delivery to B16 cells. RGD-containing peptides are known to serve as recognition motifs for multiple integrin ligands (24,25) and have been extensively utilized for drug targeting to tumor endothelial cells or metastatic tumor cells (26–29). The B16F10 murine cells are highly metastatic melanoma cells and overexpress multiple integrin-related receptors on their surface (30,31). Therefore, our observation on enhanced uptake of DOX as part of GRGDS decorated micelles compared to their acetal counterparts by B16F10 cells is not surprising (Fig. 3). The cellular uptake for the GRGDS micelles led to their localization in endosomes where more rapid release of DOX from its multifunctional polymeric micellar carriers was expected (Fig. 4). Incubation of B16F10 cells with GRGDS decorated micelles also resulted in higher levels of DOX in cell nucleus for both PEO-*b*-PBCL and PEO-*b*-P(CL-DOX) micelles (Fig. 3B-a and c) compared to their acetal-counterparts (Fig. 3B-b and d). The observation may be attributed to the rapid uptake and localization of GRGDS-decorated micelles in endosome/lysosomes of B16F10 cells, followed by facilitated core degradation and preferential release of DOX or DOX derivatives in endosomal pH, subsequent drug transfer to cytoplasm and partitioning through the nuclear membrane. Although the extracellular DOX leakage from the micelles may partly be responsible for the nuclear distribution of physically encapsulated DOX (Fig. 2A), the difference between the distribution pattern of physically encapsulated DOX and free DOX (Fig. 3B-b and d versus e) clearly shows this mechanism not to be exclusively responsible for the interaction of encapsulated DOX and cells. Perhaps, part of encapsulated DOX will remain inside the micelles, get released inside the cells after micellar uptake and gradually penetrate to the cell nucleus.

We also weighed on the potential significance of RGD modification in systems containing physically encapsulated DOX over those with chemically conjugated DOX. Overall, RGD modification appeared to affect the cellular internalization and intracellular distribution of chemically conjugated DOX to higher extent (Figs. 3 and 4). Without RGD modification, cellular uptake, endosomal or nuclear localization was either low or undetectable within 4 h of incubation. Modification of micelles with RGD ligand drastically changed this pattern. Conjugated DOX in RGD modified micelles was mainly localized in the endosomes and was also detected in the nucleus within 4 h. Cellular uptake of DOX physically loaded in either acetal- or GRGDS- decorated PEO-*b*-PBCL micelles was closer to that of free DOX when compared to chemically conjugated DOX reflecting release of physically encapsulated DOX from its carrier through diffusion into the extracellular space at physiological pH as expected and subsequent partitioning of released DOX to intracellular environment through cell membrane diffusion. This was also evident from the results of cell localization experiments, where lower endosomal localization (Fig. 3) and higher nuclear accumulation (Fig. 4) was observed for physically encapsulated DOX compared to chemically conjugated DOX in polymeric micelles.

The results of cytotoxicity studies agreed well with those of cell uptake, intracellular localization and biodegradation studies. For instance, consistent with its lower cellular uptake and nuclear localization, chemically conjugated DOX demonstrated less cytotoxicity against B16F10 cells in comparison to physically encapsulated DOX (Fig. 5). Previous studies on the *in vitro* efficacy of polymer-DOX conjugates have shown similar trend (32–34). By GRGDS modification, the cellular uptake, nuclear localization and cytotoxicity of chemically conjugated DOX were improved. In addition, decoration of polymeric micelles with GRGDS appeared more efficient in improving the cytotoxicity of conjugated DOX at longer incubation times (48 h), while this strategy seem to provide better cytotoxic effects for the physically encapsulated DOX at earlier time points (24 h). This is due to the involvement of pH triggered diffusion of physically encapsulated DOX, which enhances DOX release from micelles containing PBCL core at early time points after endosomal localization. For chemically conjugated DOX, release of DOX derivatives will depend on degradation of poly(ester) core at endosomal pH, which is a slower process than diffusion. Besides, endosomal pH triggered degradation of P(CL-DOX) core will lead to the release of DOX-HA derivatives that may undergo further degradation of the amide linkage between DOX and poly(ester) backbone (which is an even slower process) to provide free DOX. Better results in terms of cytotoxicity for RGD decorated PEO-*b*-poly(ester) based DOX conjugates may be expected if DOX is attached to the PCCL backbone through an acid cleavable hydrazone bond instead of more stable amide linkage. On balance, a better therapeutic index for RGD-modified PEO-*b*-P(CL-DOX) micellar conjugates compared to RGD-PEO-*b*-PBCL micelles containing physically encapsulated DOX in biological system is envisioned since the former is expected to prevent premature drug leakage from the carrier in a biological system and is more susceptible to changes of pH for triggered drug release. To test this hypothesis, *in vivo* studies to evaluate the RGD-modified micelles containing chemically and physically incorporated DOX are undergoing in our lab. The results of *in vivo* studies should also shed light on the efficacy of prepared multifunctional polymeric micelles for selective drug delivery to integrin overexpressing cells.

CONCLUSION

The results of this study shows a great potential for RGD modified PEO-*b*-poly(ester) based micellar DOX conjugates and containers for pH triggered enhanced intracellular drug delivery to metastatic tumor cells. Final conclusion on the success of the present multifunctional polymeric micellar drug conjugates and containers and possible superiority of one over the other in enhancing the selective delivery of encapsulated drug can only be made only by *in vivo* studies.

ACKNOWLEDGEMENTS

This study was supported by the Natural Sciences and Engineering Council of Canada (NSERC) grant Nos. G121210926 and G121220086. AM was supported by Rx and D HRF/CIHR graduate student research scholarship.

REFERENCES

1. R. Duncan. Polymer conjugates as anticancer nanomedicines. *Nat. Rev.* **6**:688–701 (2006).
2. R. Duncan. The dawning era of polymer therapeutics. *Nat. Rev.* **2**:347–360 (2003).
3. M. Ferrari. Cancer nanotechnology: opportunities and challenges. *Nat. Rev. Cancer.* **5**:161–171 (2005) doi:10.1038/nrc1566.
4. A. Mahmud, X. B. Xiong, and A. Lavasanifar. Novel self-associating poly(ethylene oxide)-block-poly(epsilon-caprolactone) block copolymers with functional side groups on the polyester block for drug delivery. *Macromolecules.* **39**:9419–9428 (2006) doi:10.1021/ma0613786.
5. A. Lavasanifar, J. Samuel, and G. S. Kwon. Poly(ethylene oxide)-block-poly(L-amino acid) micelles for drug delivery. *Adv. Drug Deliv. Rev.* **54**:169–190 (2002) doi:10.1016/S0169-409X(02)00015-7.
6. K. Kataoka, A. Harada, and Y. Nagasaki. Block copolymer micelles for drug delivery: design, characterization and biological significance. *Adv. Drug Deliv. Rev.* **47**:113–131 (2001) doi:10.1016/S0169-409X(00)00124-1.
7. A. Mahmud, X. B. Xiong, H. M. Aliabadi, and A. Lavasanifar. Polymeric micelles for drug targeting. *J. Drug. Target.* **15**:553–584 (2007) doi:10.1080/10611860701538586.
8. A. Mahmud, X. B. Xiong, and A. Lavasanifar. Self-associating poly(ethylene oxide)-block-poly(epsilon-caprolactone) copolymers with carboxyl, benzyl carboxylate and doxorubicin side group: Novel micellar nano-containers and drug conjugates. *Eur. J. Pharm. Biopharm.*, in press (2008).
9. D. G. Stupackand, and D. A. Cheresh. Integrins and angiogenesis. *Curr. Top. Dev. Biol.* **64**:207–238 (2004) doi:10.1016/S0070-2153(04)64009-9.
10. J. D. Hoodand, and D. A. Cheresh. Role of integrins in cell invasion and migration. *Nat. Rev.* **2**:91–100 (2002).
11. J. A. Varnerand, and D. A. Cheresh. Integrins and cancer. *Curr. Opin. Cell Biol.* **8**:724–730 (1996) doi:10.1016/S0955-0674(96)80115-3.
12. Y. Bae, W. D. Jang, N. Nishiyama, S. Fukushima, and K. Kataoka. Multifunctional polymeric micelles with folate-mediated cancer cell targeting and pH-triggered drug releasing properties for active intracellular drug delivery. *Mol. Biosyst.* **1**:242–250 (2005) doi:10.1039/b500266d.
13. Y. Bae, N. Nishiyama, and K. Kataoka. *In vivo* antitumor activity of the folate-conjugated pH-sensitive polymeric micelle selectively releasing adriamycin in the intracellular acidic compartments. *Bioconjug. Chem.* **18**:1131–1139 (2007) doi:10.1021/bc060401p.
14. N. D. Scott, J. F. Walker, and V. L. Hansley. Sodium naphthalene I A new method for the preparation of addition compounds of alkali metals and polycyclic aromatic hydrocarbons. *J. Am. Chem. Soc.* **58**:2442–2444 (1936) doi:10.1021/ja01303a022.
15. C. Scholz, M. Iijima, Y. Nagasaki, and K. Kataoka. A novel reactive polymeric micelle with aldehyde groups on its surface. *Macromolecules.* **28**:7295–7297 (1995) doi:10.1021/ma00125a040.
16. A. Mahmudand, and A. Lavasanifar. The effect of block copolymer structure on the internalization of polymeric micelles by human breast cancer cells. *Colloids. Surf. B. Biointerfaces.* **45**:82–89 (2005) doi:10.1016/j.colsurfb.2005.07.008.
17. X. B. Xiong, A. Mahmud, H. Uludag, and A. Lavasanifar. Conjugation of arginine-glycine-aspartic acid peptides to poly(ethylene oxide)-b-poly(epsilon-caprolactone) micelles for enhanced intracellular drug delivery to metastatic tumor cells. *Biomacromolecules.* **8**:874–884 (2007) doi:10.1021/bm060967g.
18. A. Lavasanifar, J. Samuel, and G. S. Kwon. The effect of alkyl core structure on micellar properties of poly(ethylene oxide)-block-poly(L-aspartamide) derivatives. *Colloids. Surf. B. Biointerfaces.* **22**:115–126 (2001) doi:10.1016/S0927-7765(01)00147-3.
19. R. Karinaga, K. Koumoto, M. Mizu, T. Anada, S. Shinkai, and K. Sakurai. PEG-appended beta-(1->3)-D-glucan schizophyllan to deliver antisense-oligonucleotides with avoiding lysosomal degradation. *Biomaterials.* **26**:4866–4873 (2005) doi:10.1016/j.biomaterials.2004.11.031.
20. M. Oba, S. Fukushima, N. Kanayama, K. Aoyagi, N. Nishiyama, H. Koyama, and K. Kataoka. Cyclic RGD peptide-conjugated polyplex micelles as a targetable gene delivery system directed to cells possessing alpha(v)beta(3) and alpha(v)beta(5) Integrins. *Bioconjug. Chem.* **18**:1415–1423 (2007).
21. Y. Yamamoto, Y. Nagasaki, M. Kato, and K. Kataoka. Surface charge modulation of poly(ethylene glycol)-poly(D, L-lactide) block copolymer micelles: conjugation of charged peptides. *Colloid. Surface B.* **16**:135–146 (1999) doi:10.1016/S0927-7765(99)00065-X.
22. Y. Gengand, and D. E. Discher. Hydrolytic degradation of poly(ethylene oxide)-block-polycaprolactone worm micelles. *J. Am. Chem. Soc.* **127**:12780–12781 (2005) doi:10.1021/ja053902e.
23. G. S. Kwon, M. Yokoyama, T. Okano, Y. Sakurai, and K. Kataoka. Biodistribution of micelle-forming polymer-drug conjugates. *Pharm. Res.* **10**:970–974 (1993) doi:10.1023/A:1018998203127.
24. R. Pasqualini, E. Koivunen, and E. Ruoslahti. Peptides in cell adhesion: powerful tools for the study of integrin-ligand interactions. *Braz. J. Med. Biol. Res.* **29**:1151–1158 (1996)
25. E. Ruoslahti. RGD and other recognition sequences for integrins. *Annu. Rev. Cell. Dev. Biol.* **12**:697–715 (1996) doi:10.1146/annurev.cellbio.12.1.697.
26. N. Nasongkla, X. Shuai, H. Ai, B. D. Weinberg, J. Pink, D. A. Boothman, and J. Gao. cRGD-functionalized polymer micelles for targeted doxorubicin delivery. *Angew. Chem. Int. Ed. Engl.* **43**:6323–6327 (2004) doi:10.1002/anie.200460800.
27. X. B. Xiong, Y. Huang, W. L. Lu, X. Zhang, H. Zhang, T. Nagai, and Q. Zhang. Enhanced intracellular delivery and improved antitumor efficacy of doxorubicin by sterically stabilized liposomes modified with a synthetic RGD mimetic. *J. Control Release.* **107**:262–275 (2005) doi:10.1016/j.jconrel.2005.03.030.
28. X. B. Xiong, Y. Huang, W. L. Lu, H. Zhang, X. Zhang, and Q. Zhang. Enhanced intracellular uptake of sterically stabilized liposomal Doxorubicin *in vitro* resulting in improved antitumor activity *in vivo*. *Pharm. Res.* **22**:933–939 (2005) doi:10.1007/s11095-005-4588-x.
29. W. Arap, R. Pasqualini, and E. Ruoslahti. Cancer treatment by targeted drug delivery to tumor vasculature in a mouse model. *Science.* **279**:377–380 (1998) doi:10.1126/sci.ence.279.5349.377.
30. K. D. Cowden Dahl, S. E. Robertson, V. M. Weaver, and M. C. Simon. Hypoxia-inducible factor regulates alphavbeta3 integrin cell surface expression. *Mol. Biol. Cell.* **16**:1901–1912 (2005) doi:10.1091/mbc.E04-12-1082.
31. M. J. Humphries, K. M. Yamada, and K. Olden. Investigation of the biological effects of anti-cell adhesive synthetic peptides that inhibit experimental metastasis of B16-F10 murine melanoma cells. *J. Clin. Invest.* **81**:782–790 (1988) doi:10.1172/JCI113384.
32. M. Yokoyama, M. Miyauchi, N. Yamada, T. Okano, Y. Sakurai, K. Kataoka, and S. Inoue. Characterization and anticancer activity of the micelle-forming polymeric anticancer drug adriamycin-conjugated poly(ethylene glycol)-poly(aspartic acid) block copolymer. *Cancer Res.* **50**:1693–1700 (1990).
33. F. Greco, M. J. Vicent, S. Gee, A. T. Jones, J. Gee, R. I. Nicholson, and R. Duncan. Investigating the mechanism of enhanced cytotoxicity of HPMA copolymer-Dox-AGM in breast cancer cells. *J. Control Release.* **117**:28–39 (2007) doi:10.1016/j.jconrel.2006.10.012.
34. Y. Luo, N. J. Bernshaw, Z. R. Lu, J. Kopecek, and G. D. Prestwich. Targeted delivery of doxorubicin by HPMA copolymer-hyaluronan bioconjugates. *Pharm. Res.* **19**:396–402 (2002) doi:10.1023/A:1015170907274.